Published in J Cell Sci doi: 10.1242/jcs.198382, 2017
which should be cited to refer to this work.

Ypk1/Ypk2 kinases maintain Rho1 at the plasma membrane by flippase-dependent lipid remodelling after membrane stresses

Authors:

Riko Hatakeyama[1, 2*], Keiko Kono[3] and Satoshi Yoshida[1, 4, 5*]

Affiliations:

[1]Department of Biology and Rosenstiel Basic Biomedical Research Center, Brandeis University, 415 South Street, Waltham, MA, 02454 USA

[2]Department of Biology, University of Fribourg, Chemin du Musée 10, CH-1700 Fribourg, Switzerland

[3]Department of Cell Biology, Graduate School of Medical Sciences, Nagoya City University, 1 Kawasumi, Mizuho-cho, Mizuho-ku, Nagoya 467-8601, Japan

[4]Gunma Initiative for Advanced Research (GIAR), Gunma University, Gunma, Japan

[5]Institute for Molecular and Cellular Regulation, Gunma University, Gunma, Japan

Contacts:

*riko.hatakeyama@unifr.ch or satoshi@gunma-u.ac.jp

Key words:

Akt, Rho, flippase, phosphatidylserine, membrane stress, actin cytoskeleton

Abbreviations

PM, plasma membrane

TORC2, target of rapamycin complex 2

PS, phosphatidylserine

PE, phosphatidylethanolamine

$PI(4,5)P_2$, phosphatidylinositol 4,5-bisphosphate

PBS, polybasic sequence

GEF, guanine nucleotide exchange factor

PH, pleckstrin homology

GDI, guanine nucleotide dissociation inhibitor

PKC, protein kinase C

PLC, phospholipase C

DAG, diacylglycerol

IP_3, inositol triphosphates

Summary statement

Yeast resists to plasma membrane stress by maintaining cortical localization of Rho GTPase via Ypk kinase and flippase-mediated lipid remodelling.

Abstract

The plasma membrane (PM) is frequently challenged by mechanical stresses. In budding yeast, TORC2-Ypk1/Ypk2 kinase cascade plays a critical role in PM stress responses by reorganizing the actin cytoskeleton via Rho1 GTPase. However, the molecular mechanism by which TORC2-Ypk1/Ypk2 regulates Rho1 is not well defined. Here, we found that Ypk1/Ypk2 maintain PM localization of Rho1 under PM stress via spatial reorganization of the lipids including phosphatidylserine (PS). Genetic evidence suggests that this process is mediated by the Lem3-containing lipid flippase. We propose that TORC2-Ypk1/Ypk2-Lem3 axis-mediated lipid remodelling is a backup mechanism for PM anchoring of Rho1 after PM stress-induced acute degradation of phosphatidylinositol 4,5-bisphosphate ($PI(4,5)P_2$), which is responsible for Rho1 localization in a normal condition. Since all the signaling molecules studied here are conserved in higher eukaryotes, our findings may represent a general mechanism to cope with PM stress.

Introduction

The plasma membrane (PM) frequently suffers from physical stress, including turgor pressure caused by imbalanced osmolality and membrane stretching/shrinking caused by muscle contraction (Lessey et al, 2012; Hohmann, 2002). Moreover, abnormal lipid composition causes PM stress even without environmental perturbations (Berchtold et al, 2012). To quickly manage such PM stress, eukaryotic cells have developed sophisticated signalling circuits involving the target of rapamycin complex 2 (TORC2) kinase complex. TORC2 is activated by PM stress such as hypotonic shock or inhibition of sphingolipid biosynthesis (Berchtold et al, 2012) and regulates various cellular functions, including actin organization, cell motility and morphogenesis (Loewith and Hall, 2011; Cybulski and Hall, 2009; Loewith et al, 2002; Zoncu et al, 2011).

In both yeast and mammals, the Rho-family of GTPases is a critical target of TORC2 (Schmidt et al, 1997; Jacinto et al, 2004; Ho et al, 2008; Helliwell et al, 1998). In budding yeast, the RhoA homolog Rho1 plays essential roles in actin organization and in stress responses (Levin, 2011). After activation by its guanine nucleotide exchange factors (GEFs), Rho1 binds to and recruits its effector Pkc1 (Andrews and Stark, 2000; Kamada et al, 1996), the only protein kinase C (PKC) in budding yeast, to the PM. Then, Rho1-GTP and the membrane lipid phosphatidylserine (PS) cooperatively activate Pkc1 (Kamada et al, 1996), which in turn activates the downstream MAP kinase cascade for transcriptional responses (Kamada et al, 1995) and remodels actin organization partly through down-regulation of the formin Bni1 and the exocyst subunit Sec3 (Kono et al, 2012). Several models have been proposed to explain how TORC2 regulates Rho1 and Pkc1, including TORC2-dependent activation of Rho1 GEFs (Schmidt et al, 1997; Ho et al, 2008) and Pkc1 phosphorylation by TORC2 (Nomura and Inoue, 2015). However, the physiological significance of these mechanisms is not well understood.

The best-characterized TORC2 target is the Akt/SGK family of protein kinases, which are directly phosphorylated and activated by TORC2 (Kamada et al, 2005). The yeast Akt/SGK homologs Ypk1/Ypk2 regulate sphingolipid synthesis via Orm1/Orm2 and Lac1/Lag1 (Roelants et al, 2011; Muir et al, 2014; Sun et al, 2012; Aronova et al, 2008), phospholipid flipping via the flippase kinases Fpk1/Fpk2 (Roelants et al, 2010), and production and efflux of glycerol via Gpd1 and Fps1, respectively (Lee et al, 2012; Muir et al, 2015). Among these effectors, Fpk1/Fpk2, whose kinase activities are inhibited by phosphorylation by Ypk1/Ypk2 (Roelants et al, 2010), are of particular importance because a recent quantitative phosphoproteomic approach revealed that regulation of actin polarization and endocytosis by the TORC2-Ypk1/Ypk2 pathway is largely mediated by the Fpk1/Fpk2 axis (Rispal et al, 2015). A recent study demonstrated that Fpk1/Fpk2 negatively regulate the Rho1-Pkc1 pathway, at least in part via the Rho1 GEF Rom2 (Niles and Powers, 2014). However, the Fpk1/Fpk2 substrates that regulate Rho1-Pkc1 remain unknown.

In this study, we define a key signalling mechanism linking the TORC2-Ypk1/Ypk2-Fpk1/Fpk2 kinase cascade to Rho1-Pkc1. Ypk1/Ypk2 promote cortical localization of Rho1 via inhibition of the Lem3-containing lipid flippase complex, an established target of Fpk1/Fpk2. The flippase complex determines subcellular distribution of PS, which is required for Rho1 localization and cell viability under stress. We propose that Ypk1/Ypk2-dependent rearrangement of PS compensates for the reduction of anionic charge at the PM caused by stress-triggered degradation of phosphatidylinositol 4,5-bisphosphate ($PI(4,5)P_2$).

Results

Ypk1/Ypk2 support Rho1 localization to the bud cortex during PM stress

The TORC2-Ypk1/Ypk2 cascade regulates actin polarity (Rispal et al, 2015). To examine the relationship between *YPK1/YPK2* and *RHO1*, we first tested their genetic interaction. Overexpression of *RHO1* rescued the temperature-sensitive (ts) growth defect of the *ypk1-1 ypk2Δ* strain (hereafter referred to as ypk^{ts}) (Fig. 1A). Moreover, the actin organization defect of ypk^{ts} cells was largely rescued by overexpression of *RHO1* (Fig 1B). These results suggest that Ypk1/Ypk2 regulate actin organization via or in parallel with Rho1.

TORC2 activates Rho1 GEFs by an unknown mechanism (Schmidt et al, 1997; Ho et al, 2008), and Fpk1/Fpk2 regulates the localization of the Rho1 GEF Rom2 (Niles and Powers, 2014). If Ypk1/Ypk2 regulate Rho1 solely via GEFs, then active mutants of Rho1 would rescue ypk^{ts}. To test this possibility, we expressed two Rho1 active forms in ypk^{ts} cells: *RHO1-Q68H* mutant, which is defective in GTP hydrolysis, and *RHO1-F35L* mutant, which has high intrinsic nucleotide exchange activity. These *RHO1* mutants are dominantly active and rescue the lethality of the cells lacking all three Rho1 GEFs, Rom1, Rom2 and Tus1 (Yoshida et al, 2009). Neither of these Rho1 active mutations suppressed the ypk^{ts} growth defect (Fig. 1C). A plausible interpretation of these results is that Ypk1/Ypk2 regulates Rho1 through GEF-independent mechanisms.

Next, we tested the possibility that Ypk1/Ypk2 regulate Rho1 localization. In wild type cells, Rho1 is concentrated at the bud cortex during polarized growth. We found that localization of GFP-Rho1 at the bud cortex was slightly reduced in ypk^{ts} cells at the restrictive temperature, although Rho1 protein was expressed at a normal level (Fig. 1D, E). Ypk1/Ypk2 are activated upon PM stresses, such as hypotonic shock or treatment with myriocin (an inhibitor of sphingolipid synthesis) and are essential for the resistance to these stresses (Berchtold et al, 2012). Based on these notions, we examined GFP-Rho1 localization under these stresses. In both stressed conditions, ypk^{ts} cells showed more prominent impairment

of cortical localization of Rho1 than when unstressed (Fig. 1D, F). These results suggest that Ypk1/Ypk2 support PM localization of Rho1, especially when the PM is stressed.

Ypk1/Ypk2 regulate subcellular distribution of PS

Rho GTPases Rho1 and Cdc42 are delivered to the inner cortex of growing daughter cell tip via polarized secretion (Wedlich-Soldner et al, 2003; Abe et al, 2003). Once delivered, Rho1 and Cdc42 are anchored to the inner PM by two mechanisms: hydrophobic interaction with the PM via covalently attached geranylgeranyl moiety and electrostatic interaction with anionic PM lipids via poly-basic sequences (PBS) (Heo et al, 2006). Therefore, elaborate regulation of anionic lipids is essential for stable localization of Rho1. Although Ypk1/Ypk2 are well-established regulators of sphingolipids and neutral glycerophospholipids (Roelants et al, 2010; Roelants et al, 2011; Muir et al, 2014; Sun et al, 2012; Aronova et al, 2008), it is unclear if and how anionic lipids are regulated by Ypk1/Ypk2.

We have previously shown that Rho1 localizes to the PM in part by interaction of Rho1 PBS located in the C-terminal region with $PI(4,5)P_2$ (Yoshida et al, 2009). Therefore, we first tested the role of Ypk1/Ypk2 in $PI(4,5)P_2$ regulation. GFP-$2PH^{PLC}$, a specific biosensor for $PI(4,5)P_2$ (Stefan et al, 2002), exclusively decorated the PM in both wild type and *ypk*^{ts} cells (Fig. 2A), suggesting that Ypk1/Ypk2 are not required to maintain $PI(4,5)P_2$ levels.

Next, we examined the role of Ypk1/Ypk2 in subcellular distribution of PS, another major anionic lipid, using the specific PS biosensor GFP-$2PH^{evt-2}$ (Uchida et al, 2011; Lee et al, 2015). PS is implicated in polarized growth via PM recruitment of the Rho GTPase Cdc42 in both yeast and humans (Fairn et al, 2011; Das et al, 2012; Bruurs et al, 2015). GFP-$2PH^{evt-2}$ showed peripheral localization in wild type cells, reflecting enrichment of PS at the inner leaflet of the PM (Fig. 2B). In sharp contrast, GFP-$2PH^{evt-2}$ was severely lost from the PM and relocated to the early endosomes in *ypk*^{ts} cells (Fig. 2B, C). Similar relocation of GFP-$2PH^{evt-2}$ was observed in *ypk1(L424A) ypk2Δ*, the analog-sensitive *ypk* mutant (Roelants et al, 2011)

(Fig. 2D). Displacement of GFP-2PH^{evt-2} from the PM suggests either the reduction in the total amount of PS at the inner PM or impaired ability of PS to recruit GFP-2PH^{evt-2}. The latter event can be caused by an altered lateral distribution of PS, as recent evidence suggested that the nanoclustering of PS at the inner PM increases its ability to recruit proteins such as human K-Ras (Zhou et al, 2015). In either case, our data suggests that Ypk1/Ypk2 regulate spatial organization of PS.

Ypk1/Ypk2-dependent flippase inhibition is required for PS organization and Rho1 localization

Next, we sought the Ypk1/Ypk2 effector(s) of PS regulation. Ypk1/Ypk2 regulate phospholipid asymmetry by inhibiting Fpk1/Fpk2 kinases (Roelants et al, 2010). Fpk1/Fpk2 phosphorylate and activate the Dnf1/Dnf2-Lem3 lipid flippase complex, which flips the neutral lipids phosphatidylcholine (PC) and phosphatidylethanolamine (PE) from the outer leaflet to the inner leaflet of the PM (Nakano et al, 2008; Saito et al, 2004; Kato et al, 2002; Baldridge and Graham, 2012; Baldridge et al, 2013; Baldridge and Graham, 2013; Panatala et al, 2015; Iwamoto et al, 2004). In human cells, PC flipping is proposed to dilute the local concentration of PS at the inner PM (Miyano et al, 2016). We therefore examined the involvement of the flippase complex in PS regulation. We found that deletion of *LEM3* largely restores PM localization of the PS probe GFP-2PH^{evt-2} in *ypk^{ts}* (Fig. 3A). This result suggests that Ypk1/Ypk2 regulate PS distribution via inhibition of the Lem3-containing flippase complex.

We also found that *LEM3* deletion efficiently rescues delocalization of GFP-Rho1 upon hypotonic shock or myriocin treatment, as well as temperature sensitive growth defects and myriocin hypersensitivity of *ypk^{ts}* (Fig. 3B, C, D), raising the possibility that redistribution of PS might contribute to Rho1 regulation by Ypk1/Ypk2. To test the requirement of PS in Rho1 regulation, we depleted cellular PS by deleting *CHO1*, the only

gene encoding PS synthase in budding yeast. GFP-Rho1 was excessively enriched in the bud cortex in unstressed *lem3Δ* cells, whereas *CHO1* deletion cancelled this effect (Fig. 3E). Furthermore, in *lem3Δ* cells, GFP-Rho1 was maintained in the bud cortex even after myriocin treatment; this phenotype was also suppressed by *CHO1* deletion (Fig. 3F). Thus, PS is required for the flippase inhibition-dependent cortical localization of Rho1.

We further analysed the mechanism of Rho1 regulation by Lem3. PS supports cortical localization of yeast Cdc42 by preventing its extraction by Rho guanine nucleotide dissociation inhibitor (GDI) (Das et al, 2012). Rho GDI is potentially involved in flippase-mediated Rho1 regulation as well, as enhancement of PM localization of Rho1 by *LEM3* deletion was not significant in *rdi1Δ* cells, which lack the only Rho GDI in budding yeast (Fig. 3G). A recent study revealed that Ypk1/Ypk2 maintain the Rho1 GEF Rom2 at the PM via Fpk1/Fpk2 inhibition (Niles and Powers, 2014), suggesting that Rom2 might contribute to Rho1 regulation by Ypk1/Ypk2. However, enhanced PM localization of Rho1 in by *LEM3* deletion was still evident in the yeast strains lacking all three Rho1 GEFs, Rom1, Rom2 and Tus1 (*ΔGEF*) (Fig. 3H), suggesting that Rho1 regulation by flippase is not solely mediated by GEFs.

Next, we examined whether Rho1 physically associates with PS. An in vitro binding assay using PIP strips indicated that Rho1 PBS have an affinity for PS, supporting the idea that PS contributes to the cortical localization of Rho1 via electrostatic interaction, although the interaction was weaker than that of other anionic lipids (Fig. 3I). In vivo, high concentration of PS at the PM may compensate for the low affinity of PS to Rho1 PBS, as PS accounts for more than 10% of PM phospholipids, whereas $PI(4,5)P_2$ composes only 1% (Fairn and Grinstein, 2012; Leventis and Grinstein, 2010; van et al, 2008; Martin, 2015). Nanoclustering of PS at the PM might also contribute to Rho1 binding, as is the case for human K-Ras (Zhou et al, 2015). We confirmed that the effect of *lem3Δ* on Rho1 PM localization in vivo is mediated by the PBS, as the $Rho1^{5KA}$ mutant, whose five lysines in the

PBS are mutated to alanine (Yoshida et al, 2009), did not accumulate in the PM in *lem3Δ* cells (Fig. 3J). Taken together, our data supports the model that flippase inhibition by Ypk1/Ypk2 promotes PM localization of Rho1 by enhancing the electrostatic interaction between Rho1 PBS and anionic lipids, including PS.

PS is essential for Rho1 localization and recovery from PM stress

As PS is a highly abundant anionic lipid composing up to 10% of PM phospholipids (Fairn and Grinstein, 2012; Leventis and Grinstein, 2010; van et al, 2008), its contribution to the net negative charge of the PM is significant. Interestingly, however, the *cho1Δ* mutant is viable, indicating that PS is dispensable for normal cell proliferation. Based on our finding that PS is under the control of Ypk1/Ypk2 (Fig. 2), we speculated that PS might play an important role under PM stress. To test this hypothesis, we examined GFP-Rho1 localization in the *cho1Δ* mutant under PM stress. In *cho1Δ* cells, GFP-Rho1 normally localized to the PM in the unstressed condition. In contrast, upon hypotonic shock, cortical GFP-Rho1 localization was severely impaired (Fig. 4A). Because PS is a precursor of PE, *CHO1* deletion also significantly decreases the level of PE (Fairn et al, 2011). To rule out the possibility that defective GFP-Rho1 localization in *cho1Δ* cells is an indirect consequence of PE reduction, we examined Rho1 localization in the *psd1Δ* mutant, which lacks the major PE synthase (Trotter et al, 1993). Regardless of stress, *psd1Δ* cells were only slightly defective in the cortical localization of GFP-Rho1, suggesting that PE may have a minor role in Rho1 localization (Fig. 4B). Importantly, hypotonic shock did not cause severe delocalization of GFP-Rho1 in *psd1Δ* cells. Thus, the loss of cortical Rho1 localization in *cho1Δ* cells under PM stress is not due to the loss of PE. Analogous to hypotonic shock, Rho1 delocalization induced by myriocin treatment was exacerbated in *cho1Δ* cells (Fig. 4C). These results suggest that PS is critical for the maintenance of cortical Rho1 localization, specifically under PM stress.

Rho1 recruits its effector protein Pkc1 to the bud cortex (Andrews and Stark, 2000). Analogous to GFP-Rho1, delocalization of Pkc1-GFP after myriocin treatment was more prominent in *cho1Δ* cells and milder in *lem3Δ* cells (Fig. S1), suggesting that PS ensures not only localization but also function of Rho1 under PM stress.

Delocalization of Pkc1-GFP in *cho1Δ* cells raised the possibility that phosphorylation of Mpk1, the major downstream factor of Pkc1 signalling pathway, could be decreased in these cells. However, phosphorylation of Mpk1 in response to hypotonic shock was observed even in *cho1Δ* cells (data not shown). This suggests that localization of Pkc1 to the bud cortex is not necessarily essential for stress-triggered activation of the downstream MAP kinase cascade, consistent with the recent observation that Pkc1 can activate the MAP kinase cascade even at endosomes when $PI(4,5)P_2$ is artificially eliminated (Fernandez-Acero et al, 2015). It is possible that PS-dependent regulation of Rho1-Pkc1 axis is critical for Pkc1 targets other than the MAP kinase cascade. As an alternative readout of Rho1-Pkc1 function, we examined organization of the actin cytoskeleton, a defect associated with Rho1-Pkc1 malfunction (Delley and Hall, 1999), in *cho1Δ* cells. In normal growth conditions, yeast actin cytoskeleton polarizes at the small to medium-sized buds to sustain polarized bud growth (Pruyne and Bretscher, 2000; Moseley and Goode, 2006). Under conditions such as heat shock or cell wall damages, the actin cytoskeleton is rapidly depolarized to suspend polarized cell growth and to repair damage (Levin, 2011). Consistent with a recent report (Gualtieri et al, 2004), upon transient (20 min) hypotonic shock, the cortical actin cytoskeleton was rapidly depolarized and eventually repolarized within 3 hours in wild type cells (Fig. 4D). The actin repolarization process required Pkc1 activity, as *pkc1-2* temperature-sensitive mutant cells failed to repolarize actin 3 hours after hypotonic shock (Fig. 4D). We found that *cho1Δ* cells showed an even more severe actin depolarization phenotype than *pkc1-2* cells. Furthermore, *cho1Δ* cells failed to repolarize even after three

hours (Fig. 4D), suggesting requirement of PS for rapid repolarization and/or the completion of repair processes.

Then, we monitored cell proliferation after hypotonic shock. After the shock, wild type cells exhibited only a transient growth arrest (less than one hour) (Fig. 4E). In contrast, both *pkc1-2* and *cho1Δ* cells failed to proliferate for at least 5 hours after release from the shock (Fig. 4E). This was not simply due to cell death or lysis because these cells remained viable and eventually restarted growth in 24 hours (Fig. S2). The *psd1Δ* strain restarted growth within one hour, which was comparable to the recovery time for wild type cells (data not shown), excluding the possibility that the growth recovery defects in *cho1Δ* are due to the loss of PE. These results suggest that PS and Pkc1 are required for recovery after hypotonic shock.

We found *cho1Δ* cells were highly sensitive to PM stress induced by myriocin treatment but not *psd1Δ* cells (Fig. 4F). The myriocin sensitivity of *cho1Δ* cells is likely due to the loss of PS but not PE, as the *psd1Δ* mutant was not hypersensitive to myriocin (Fig. 4F). In contrast to *cho1Δ* cells, *lem3Δ* cells were resistant to myriocin, similarly to the flippase mutant *dnf1Δ dnf2Δ dnf3Δ* (Roelants et al, 2010). Myriocin resistance in the *lem3Δ* strain was largely cancelled by *CHO1* deletion but not by *PSD1* deletion (Fig. 4F), confirming the contribution of PS, but not PE, to PM stress resistance.

Genetic evidence suggests that one of the critical targets of PS in the PM stress response is the Rho1-Pkc1 pathway: the myriocin sensitivity of *cho1Δ* cells was partially rescued by overexpressing Rho1 in presence of Pkc1-R398P, the constitutively active allele of Pkc1 (Nonaka et al, 1995) (Fig. 4G). Neither overexpression of Rho1 alone nor expression of Pkc1-R398P alone detectably rescued myriocin sensitivity, indicating that PS promotes both PM recruitment of Rho1 and activation of Pkc1 during PM stress.

Flippase inhibition ensures Rho1 localization in the absence of PI(4,5)P_2

A key question is why PS is required for Rho1 localization only when the PM is stressed (Fig. 4A). In normal conditions, PI(4,5)P_2 plays a major role in cortical localization of Rho1 (Yoshida et al, 2009). However, upon various stimuli such as mechanical stress to the PM, a large fraction (roughly 50%) of PI(4,5)P_2 is immediately degraded by phospholipase C (PLC) to produce the second messengers diacylglycerol (DAG) and inositol triphosphates (IP_3) (Storch et al, 2012; Perera et al, 2004). Based on these facts, we hypothesized that PS becomes essential only when PI(4,5)P_2 levels are reduced. Consistent with this idea, the *cho1Δ* mutant shows a synthetic growth defect in combination with the temperature-sensitive mutation of *MSS4* (Sun and Drubin, 2012), which encodes the only PI4P 5-kinase in yeast (Homma et al, 1998; Desrivieres et al, 1998).

We confirmed the rapid loss of PI(4,5)P_2 upon PM stress (Perera et al, 2004) with a visual assay using GFP-2PH^{PLC}. We observed a rapid redistribution of GFP-2PH^{PLC} from the PM into the cytoplasm within 2-4 min after hypotonic shock (Fig. 5A).

To test our hypothesis that PS compensates for PI(4,5)P_2, we examined the effect of flippase inhibition on Rho1 localization when PI(4,5)P_2 was absent. In *mss4-1* cells, Rho1 failed to localize to the PM at the restrictive temperature (Fig. 5B), confirming the requirement of PI(4,5)P_2 in Rho1 localization. However, *LEM3* deletion significantly restored Rho1 localization without detectably restoring PI(4,5)P_2 production in the *mss4-1* mutant (Fig. 5B). Both the temperature-sensitive growth defect and myriocin hypersensitivity of *mss4-1* cells were rescued by *LEM3* deletion (Fig. 5C). Collectively, our data suggest that inhibition of flippase, which is triggered by TORC2-Ypk1/Ypk2 activation, supports PM localization of Rho1 and cell survival when PI(4,5)P_2 is limited. Because enhanced Rho1 localization and myriocin resistance of *lem3Δ* cells are dependent on *CHO1* (Fig. 3D, 3E and 4F), PS should have a significant role in phenotypic rescue of *mss4-1* by *LEM3* deletion.

Discussion

Although previous genetic studies placed TORC2 upstream of the Rho1-Pkc1 pathway (Helliwell et al, 1998; Helliwell et al, 1998), the molecular link between them has been poorly understood. Here, we show that Ypk1/Ypk2, essential substrates of TORC2, regulate peripheral localization of Rho1 via flippase-mediated rearrangement of phospholipids. Our results pinpointed that PS is the key lipid responsible for Rho1 localization and function during stresses and that the spatial organization of PS is controlled largely by the Ypk1/Ypk2-flippase pathway. Based on our observations that PS is required for Rho1 localization under stress and that flippase inhibition bypasses the requirement of $PI(4,5)P_2$, we propose that Ypk1/Ypk2 redistribute PS as a backup for $PI(4,5)P_2$, thereby allowing production of $PI(4,5)P_2$-derived second messengers without abandoning Rho1-Pkc1 signalling (Fig. 5D).

The precise mechanism by which Dnf1/Dnf2-Lem3 flippase complex regulates PS distribution remains an important question. As PS is not a good substrate of Dnf1, which rather prefers PC and PE (Baldridge and Graham, 2012), PS regulation by this flippase might be a consequence of PC/PE flipping.

We note that *LEM3* deletion only partially rescued the actin polarization defect in ypk^{ts} cells (data not shown), similar to the defect after pharmacological inhibition of TORC2 (Rispal et al, 2015). Therefore, Rho1 targeting does not appear to be the only mechanism by which TORC2-Ypk1/Ypk2 pathway regulates actin organization. Further studies are needed to fully understand the role for Ypk1/Ypk2 in this process.

In animals, the PM of certain cell types, such as cardiomyocytes and smooth muscles, are regularly exposed to physical stress. Because critical roles of TORC2 and Rho-PKC pathways in cardiac function and stress response have been demonstrated (Kajimoto et al, 2011; Volkers et al, 2013; Yano et al, 2014; Sciarretta et al, 2015; Zhao et al, 2014; Moschella et al, 2013), flippases and PS may serve as key signalling mediators in these cell types as well.

Materials and methods

Yeast strains, plasmids, and media

The *Saccharomyces cerevisiae* strains used in this study are listed in Table S1. Strains were constructed using standard yeast genetics procedures (Longtine et al, 1998). Plasmids used in this study are listed in Table S2.

For experiments using plasmids, cells were grown in synthetic complete (SC) medium lacking appropriate nutrients for plasmid preservation. In experiments including the *cho1Δ* strain, 1 mM ethanolamine was added to SC medium for growth support (Hikiji et al, 1988). YPD medium was used for experiments without plasmid unless specified. Unless specified, cells were grown to mid-log phase at 30°C.

In hypotonic shock experiments, cells were acclimated to hypertonic conditions by growing them in the presence of 1 M sorbitol. The acclimated cells in mid-log phase were collected by centrifugation and re-suspended in 1/20x volume of the same medium and then diluted with a 20x volume of distilled water. For the actin staining and growth curve assay, which were performed at 40°C in order to inactivate Pkc1 in *pkc1-2* mutant, cells were collected after hypotonic shock for 20 min and re-cultured in the original medium (with 1 M sorbitol).

Fluorescence microscopy

Fluorescence images were acquired using an Eclipse E600 fluorescence microscope (Nikon) equipped with a DC350F charge-coupled device camera (Andor) and an oil 60x objective (NA 1.4). The images were captured and analysed with NIS-Elements software (Nikon).

Actin staining

Cells were fixed for 40 minutes with 4% formaldehyde (final concentration). After collecting by centrifugation, cells were stained for 30 minutes with 0.66 µM Alexa Fluor 488 phalloidin (A12379, Molecular Probes) and washed with phosphate-buffered saline.

PIP Strips assay

Yeast cells overexpressing GFP-tagged Rho1 C-terminal tail were collected in mid-log phase. Cell lysate was prepared by disrupting the cell pellet with glass beads in lysis buffer (50 mM Tris-HCl (pH 8.0), 10 mM EDTA, 100 mM NaCl, 0.5% Triton X-100, 1 mM phenylmethylsulfonyl fluoride, and Complete-Mini Protease Inhibitor Cocktail (Roche)). The PIP Strips membrane (Echelon) was blocked with 3% bovine serum albumin and incubated with cell lysate (0.5 mg/ml total protein) overnight at 4°C. The signal was detected with anti-GFP antibody (7.1 and 13.1, Roche) and anti-mouse HRP-conjugated IgG (NA931, GE Healthcare) and developed with ECL Prime (GE Healthcare).

Lysate preparation, SDS-PAGE and western blotting

Lysates were prepared as previously described (Hatakeyama et al, 2010). Briefly, cells were treated with 7.2% w/v trichloroacetic acid (final concentration), pelleted, washed with 70% ethanol, and then dissolved in 6 M urea buffer. After boiling in Laemmli SDS sample buffer, samples were subjected to regular SDS-PAGE and immunoblotting experiments.

Acknowledgements

We thank Tomohiko Taguchi and Shoken Lee for providing plasmids and insightful discussion. We thank Scott Emr, Yoshikazu Ohya, Daniel Lew, Jeremy Thorner and David Pellman for providing strains and plasmids. We thank members of the Yoshida Lab and Nan Pang for technical support and helpful discussion. This work was supported by a JSPS KAKENHI Grant Number JP16H04781 , Takeda Science Foundation, and by the joint research program of the Institute for Molecular and Cellular Regulation, Gunma University.

Author contributions

RH conceived and performed all the experiments. RH, KK and SY designed the experiments and wrote the paper.

References

Abe M, Qadota H, Hirata A and Ohya Y. 2003. Lack of GTP-bound Rho1p in secretory vesicles of Saccharomyces cerevisiae. J Cell Biol 162:85-97.

Andrews PD and Stark MJ. 2000. Dynamic, Rho1p-dependent localization of Pkc1p to sites of polarized growth. J Cell Sci 113 (Pt 15):2685-2693.

Aronova S, Wedaman K, Aronov PA, Fontes K, Ramos K, Hammock BD and Powers T. 2008. Regulation of ceramide biosynthesis by TOR complex 2. Cell Metab 7:148-158.

Baldridge RD and Graham TR. 2012. Identification of residues defining phospholipid flippase substrate specificity of type IV P-type ATPases. Proc Natl Acad Sci U S A 109:E290-8.

Baldridge RD, Xu P and Graham TR. 2013. Type IV P-type ATPases distinguish mono- versus diacyl phosphatidylserine using a cytofacial exit gate in the membrane domain. J Biol Chem 288:19516-19527.

Baldridge RD and Graham TR. 2013. Two-gate mechanism for phospholipid selection and transport by type IV P-type ATPases. Proc Natl Acad Sci U S A 110:E358-67.

Berchtold D, Piccolis M, Chiaruttini N, Riezman I, Riezman H, Roux A, Walther TC and Loewith R. 2012. Plasma membrane stress induces relocalization of Slm proteins and activation of TORC2 to promote sphingolipid synthesis. Nat Cell Biol 14:542-547.

Bruurs LJ, Donker L, Zwakenberg S, Zwartkruis FJ, Begthel H, Knisely AS, Posthuma G, van de Graaf SF, Paulusma CC and Bos JL. 2015. ATP8B1-mediated spatial organization of Cdc42 signaling maintains singularity during enterocyte polarization. J Cell Biol 210:1055-1063.

Cybulski N and Hall MN. 2009. TOR complex 2: a signaling pathway of its own. Trends Biochem Sci 34:620-627.

Das A, Slaughter BD, Unruh JR, Bradford WD, Alexander R, Rubinstein B and Li R. 2012. Flippase-mediated phospholipid asymmetry promotes fast Cdc42 recycling in dynamic maintenance of cell polarity. Nat Cell Biol 14:304-310.

Delley PA and Hall MN. 1999. Cell wall stress depolarizes cell growth via hyperactivation of RHO1. J Cell Biol 147:163-174.

Desrivieres S, Cooke FT, Parker PJ and Hall MN. 1998. MSS4, a phosphatidylinositol-4-phosphate 5-kinase required for organization of the actin cytoskeleton in Saccharomyces cerevisiae. J Biol Chem 273:15787-15793.

Fairn GD, Hermansson M, Somerharju P and Grinstein S. 2011. Phosphatidylserine is polarized and required for proper Cdc42 localization and for development of cell polarity. Nat Cell Biol 13:1424-1430.

Fairn GD and Grinstein S. 2012. Cell biology. Precursor or charge supplier? Science 337:653-654.

Fernandez-Acero T, Rodriguez-Escudero I, Molina M and Cid VJ. 2015. The yeast cell wall

integrity pathway signals from recycling endosomes upon elimination of phosphatidylinositol (4,5)-bisphosphate by mammalian phosphatidylinositol 3-kinase. Cell Signal 27:2272-2284.

Gualtieri T, Ragni E, Mizzi L, Fascio U and Popolo L. 2004. The cell wall sensor Wsc1p is involved in reorganization of actin cytoskeleton in response to hypo-osmotic shock in Saccharomyces cerevisiae. Yeast 21:1107-1120.

Hatakeyama R, Kamiya M, Takahara T and Maeda T. 2010. Endocytosis of the aspartic acid/glutamic acid transporter Dip5 is triggered by substrate-dependent recruitment of the Rsp5 ubiquitin ligase via the arrestin-like protein Aly2. Mol Cell Biol 30:5598-5607.

Helliwell SB, Schmidt A, Ohya Y and Hall MN. 1998. The Rho1 effector Pkc1, but not Bni1, mediates signalling from Tor2 to the actin cytoskeleton. Curr Biol 8:1211-1214.

Helliwell SB, Howald I, Barbet N and Hall MN. 1998. TOR2 is part of two related signaling pathways coordinating cell growth in Saccharomyces cerevisiae. Genetics 148:99-112.

Heo WD, Inoue T, Park WS, Kim ML, Park BO, Wandless TJ and Meyer T. 2006. PI(3,4,5)P3 and PI(4,5)P2 lipids target proteins with polybasic clusters to the plasma membrane. Science 314:1458-1461.

Hikiji T, Miura K, Kiyono K, Shibuya I and Ohta A. 1988. Disruption of the CHO1 gene encoding phosphatidylserine synthase in Saccharomyces cerevisiae. J Biochem 104:894-900.

Ho HL, Lee HY, Liao HC and Chen MY. 2008. Involvement of Saccharomyces cerevisiae Avo3p/Tsc11p in maintaining TOR complex 2 integrity and coupling to downstream signaling. Eukaryot Cell 7:1328-1343.

Hohmann S. 2002. Osmotic stress signaling and osmoadaptation in yeasts. Microbiol Mol Biol Rev 66:300-372.

Homma K, Terui S, Minemura M, Qadota H, Anraku Y, Kanaho Y and Ohya Y. 1998. Phosphatidylinositol-4-phosphate 5-kinase localized on the plasma membrane is essential for yeast cell morphogenesis. J Biol Chem 273:15779-15786.

Iwamoto K, Kobayashi S, Fukuda R, Umeda M, Kobayashi T and Ohta A. 2004. Local exposure of phosphatidylethanolamine on the yeast plasma membrane is implicated in cell polarity. Genes Cells 9:891-903.

Jacinto E, Loewith R, Schmidt A, Lin S, Ruegg MA, Hall A and Hall MN. 2004. Mammalian TOR complex 2 controls the actin cytoskeleton and is rapamycin insensitive. Nat Cell Biol 6:1122-1128.

Kajimoto K, Shao D, Takagi H, Maceri G, Zablocki D, Mukai H, Ono Y and Sadoshima J. 2011. Hypotonic swelling-induced activation of PKN1 mediates cell survival in cardiac myocytes. Am J Physiol Heart Circ Physiol 300:H191-200.

Kamada Y, Jung US, Piotrowski J and Levin DE. 1995. The protein kinase C-activated MAP kinase pathway of Saccharomyces cerevisiae mediates a novel aspect of the heat shock response. Genes Dev 9:1559-1571.

Kamada Y, Qadota H, Python CP, Anraku Y, Ohya Y and Levin DE. 1996. Activation of yeast protein kinase C by Rho1 GTPase. J Biol Chem 271:9193-9196.

Kamada Y, Fujioka Y, Suzuki NN, Inagaki F, Wullschleger S, Loewith R, Hall MN and Ohsumi Y. 2005. Tor2 directly phosphorylates the AGC kinase Ypk2 to regulate actin polarization. Mol Cell Biol 25:7239-7248.

Kato U, Emoto K, Fredriksson C, Nakamura H, Ohta A, Kobayashi T, Murakami-Murofushi K, Kobayashi T and Umeda M. 2002. A novel membrane protein, Ros3p, is required for phospholipid translocation across the plasma membrane in Saccharomyces cerevisiae. J Biol Chem 277:37855-37862.

Kono K, Saeki Y, Yoshida S, Tanaka K and Pellman D. 2012. Proteasomal degradation resolves competition between cell polarization and cellular wound healing. Cell 150:151-164.

Lee S, Uchida Y, Wang J, Matsudaira T, Nakagawa T, Kishimoto T, Mukai K, Inaba T, Kobayashi T, Molday RS et al. 2015. Transport through recycling endosomes requires EHD1 recruitment by a phosphatidylserine translocase. EMBO J 34:669-688.

Lee YJ, Jeschke GR, Roelants FM, Thorner J and Turk BE. 2012. Reciprocal phosphorylation of yeast glycerol-3-phosphate dehydrogenases in adaptation to distinct types of stress. Mol Cell Biol 32:4705-4717.

Lessey EC, Guilluy C and Burridge K. 2012. From mechanical force to RhoA activation. Biochemistry 51:7420-7432.

Leventis PA and Grinstein S. 2010. The distribution and function of phosphatidylserine in cellular membranes. Annu Rev Biophys 39:407-427.

Levin DE. 2011. Regulation of cell wall biogenesis in Saccharomyces cerevisiae: the cell wall integrity signaling pathway. Genetics 189:1145-1175.

Loewith R, Jacinto E, Wullschleger S, Lorberg A, Crespo JL, Bonenfant D, Oppliger W, Jenoe P and Hall MN. 2002. Two TOR complexes, only one of which is rapamycin sensitive, have distinct roles in cell growth control. Mol Cell 10:457-468.

Loewith R and Hall MN. 2011. Target of rapamycin (TOR) in nutrient signaling and growth control. Genetics 189:1177-1201.

Longtine MS, McKenzie A 3rd, Demarini DJ, Shah NG, Wach A, Brachat A, Philippsen P and Pringle JR. 1998. Additional modules for versatile and economical PCR-based gene deletion and modification in Saccharomyces cerevisiae. Yeast 14:953-961.

Martin TF. 2015. PI(4,5)P-binding effector proteins for vesicle exocytosis. Biochim Biophys Acta 1851:785-793.

Miyano R, Matsumoto T, Takatsu H, Nakayama K and Shin HW. 2016. Alteration of transbilayer phospholipid compositions is involved in cell adhesion, cell spreading, and focal adhesion formation. FEBS Lett .

Moschella PC, McKillop J, Pleasant DL, Harston RK, Balasubramanian S and Kuppuswamy D. 2013. mTOR complex 2 mediates Akt phosphorylation that requires PKCepsilon in adult cardiac muscle cells. Cell Signal 25:1904-1912.

Moseley JB and Goode BL. 2006. The yeast actin cytoskeleton: from cellular function to biochemical mechanism. Microbiol Mol Biol Rev 70:605-645.

Muir A, Ramachandran S, Roelants FM, Timmons G and Thorner J. 2014. TORC2-dependent protein kinase Ypk1 phosphorylates ceramide synthase to stimulate synthesis of complex sphingolipids. Elife 3:.

Muir A, Roelants FM, Timmons G, Leskoske KL and Thorner J. 2015. Down-regulation of TORC2-Ypk1 signaling promotes MAPK-independent survival under hyperosmotic stress. Elife 4:.

Nakano K, Yamamoto T, Kishimoto T, Noji T and Tanaka K. 2008. Protein kinases Fpk1p and Fpk2p are novel regulators of phospholipid asymmetry. Mol Biol Cell 19:1783-1797.

Niles BJ and Powers T. 2014. TOR complex 2-Ypk1 signaling regulates actin polarization via reactive oxygen species. Mol Biol Cell 25:3962-3972.

Nomura W and Inoue Y. 2015. Methylglyoxal activates the target of rapamycin complex 2-protein kinase C signaling pathway in Saccharomyces cerevisiae. Mol Cell Biol 35:1269-1280.

Nonaka H, Tanaka K, Hirano H, Fujiwara T, Kohno H, Umikawa M, Mino A and Takai Y. 1995. A downstream target of RHO1 small GTP-binding protein is PKC1, a homolog of protein kinase C, which leads to activation of the MAP kinase cascade in Saccharomyces cerevisiae. EMBO J 14:5931-5938.

Panatala R, Hennrich H and Holthuis JC. 2015. Inner workings and biological impact of phospholipid flippases. J Cell Sci .

Perera NM, Michell RH and Dove SK. 2004. Hypo-osmotic stress activates Plc1p-dependent phosphatidylinositol 4,5-bisphosphate hydrolysis and inositol Hexakisphosphate accumulation in yeast. J Biol Chem 279:5216-5226.

Pruyne D and Bretscher A. 2000. Polarization of cell growth in yeast. I. Establishment and maintenance of polarity states. J Cell Sci 113 (Pt 3):365-375.

Rispal D, Eltschinger S, Stahl M, Vaga S, Bodenmiller B, Abraham Y, Filipuzzi I, Movva NR, Aebersold R, Helliwell SB et al. 2015. Target of rapamycin complex 2 regulates actin polarization and endocytosis via multiple pathways. J Biol Chem .

Roelants FM, Baltz AG, Trott AE, Fereres S and Thorner J. 2010. A protein kinase network regulates the function of aminophospholipid flippases. Proc Natl Acad Sci U S A 107:34-39.

Roelants FM, Breslow DK, Muir A, Weissman JS and Thorner J. 2011. Protein kinase Ypk1 phosphorylates regulatory proteins Orm1 and Orm2 to control sphingolipid homeostasis in Saccharomyces cerevisiae. Proc Natl Acad Sci U S A 108:19222-19227.

Saito K, Fujimura-Kamada K, Furuta N, Kato U, Umeda M and Tanaka K. 2004. Cdc50p, a

protein required for polarized growth, associates with the Drs2p P-type ATPase implicated in phospholipid translocation in Saccharomyces cerevisiae. Mol Biol Cell 15:3418-3432.

Schmidt A, Bickle M, Beck T and Hall MN. 1997. The yeast phosphatidylinositol kinase homolog TOR2 activates RHO1 and RHO2 via the exchange factor ROM2. Cell 88:531-542.

Sciarretta S, Zhai P, Maejima Y, Del Re DP, Nagarajan N, Yee D, Liu T, Magnuson MA, Volpe M, Frati G et al. 2015. mTORC2 regulates cardiac response to stress by inhibiting MST1. Cell Rep 11:125-136.

Stefan CJ, Audhya A and Emr SD. 2002. The yeast synaptojanin-like proteins control the cellular distribution of phosphatidylinositol (4,5)-bisphosphate. Mol Biol Cell 13:542-557.

Storch U, Mederos y Schnitzler M and Gudermann T. 2012. G protein-mediated stretch reception. Am J Physiol Heart Circ Physiol 302:H1241-9.

Sun Y, Miao Y, Yamane Y, Zhang C, Shokat KM, Takematsu H, Kozutsumi Y and Drubin DG. 2012. Orm protein phosphoregulation mediates transient sphingolipid biosynthesis response to heat stress via the Pkh-Ypk and Cdc55-PP2A pathways. Mol Biol Cell 23:2388-2398.

Sun Y and Drubin DG. 2012. The functions of anionic phospholipids during clathrin-mediated endocytosis site initiation and vesicle formation. J Cell Sci 125:6157-6165.

Trotter PJ, Pedretti J and Voelker DR. 1993. Phosphatidylserine decarboxylase from Saccharomyces cerevisiae. Isolation of mutants, cloning of the gene, and creation of a null allele. J Biol Chem 268:21416-21424.

Uchida Y, Hasegawa J, Chinnapen D, Inoue T, Okazaki S, Kato R, Wakatsuki S, Misaki R, Koike M, Uchiyama Y et al. 2011. Intracellular phosphatidylserine is essential for retrograde membrane traffic through endosomes. Proc Natl Acad Sci U S A 108:15846-15851.

van Meer G, Voelker DR and Feigenson GW. 2008. Membrane lipids: where they are and how they behave. Nat Rev Mol Cell Biol 9:112-124.

Volkers M, Konstandin MH, Doroudgar S, Toko H, Quijada P, Din S, Joyo A, Ornelas L, Samse K, Thuerauf DJ et al. 2013. Mechanistic target of rapamycin complex 2 protects the heart from ischemic damage. Circulation 128:2132-2144.

Wedlich-Soldner R, Altschuler S, Wu L and Li R. 2003. Spontaneous cell polarization through actomyosin-based delivery of the Cdc42 GTPase. Science 299:1231-1235.

Yano T, Ferlito M, Aponte A, Kuno A, Miura T, Murphy E and Steenbergen C. 2014. Pivotal role of mTORC2 and involvement of ribosomal protein S6 in cardioprotective signaling. Circ Res 114:1268-1280.

Yoshida S, Bartolini S and Pellman D. 2009. Mechanisms for concentrating Rho1 during cytokinesis. Genes Dev 23:810-823.

Zhao X, Lu S, Nie J, Hu X, Luo W, Wu X, Liu H, Feng Q, Chang Z, Liu Y et al. 2014. Phosphoinositide-dependent kinase 1 and mTORC2 synergistically maintain postnatal heart growth and heart function in mice. Mol Cell Biol 34:1966-1975.

Zhou Y, Wong CO, Cho KJ, van der Hoeven D, Liang H, Thakur DP, Luo J, Babic M, Zinsmaier KE, Zhu MX et al. 2015. SIGNAL TRANSDUCTION. Membrane potential modulates plasma membrane phospholipid dynamics and K-Ras signaling. Science 349:873-876.

Zoncu R, Efeyan A and Sabatini DM. 2011. mTOR: from growth signal integration to cancer, diabetes and ageing. Nat Rev Mol Cell Biol 12:21-35.

Figures

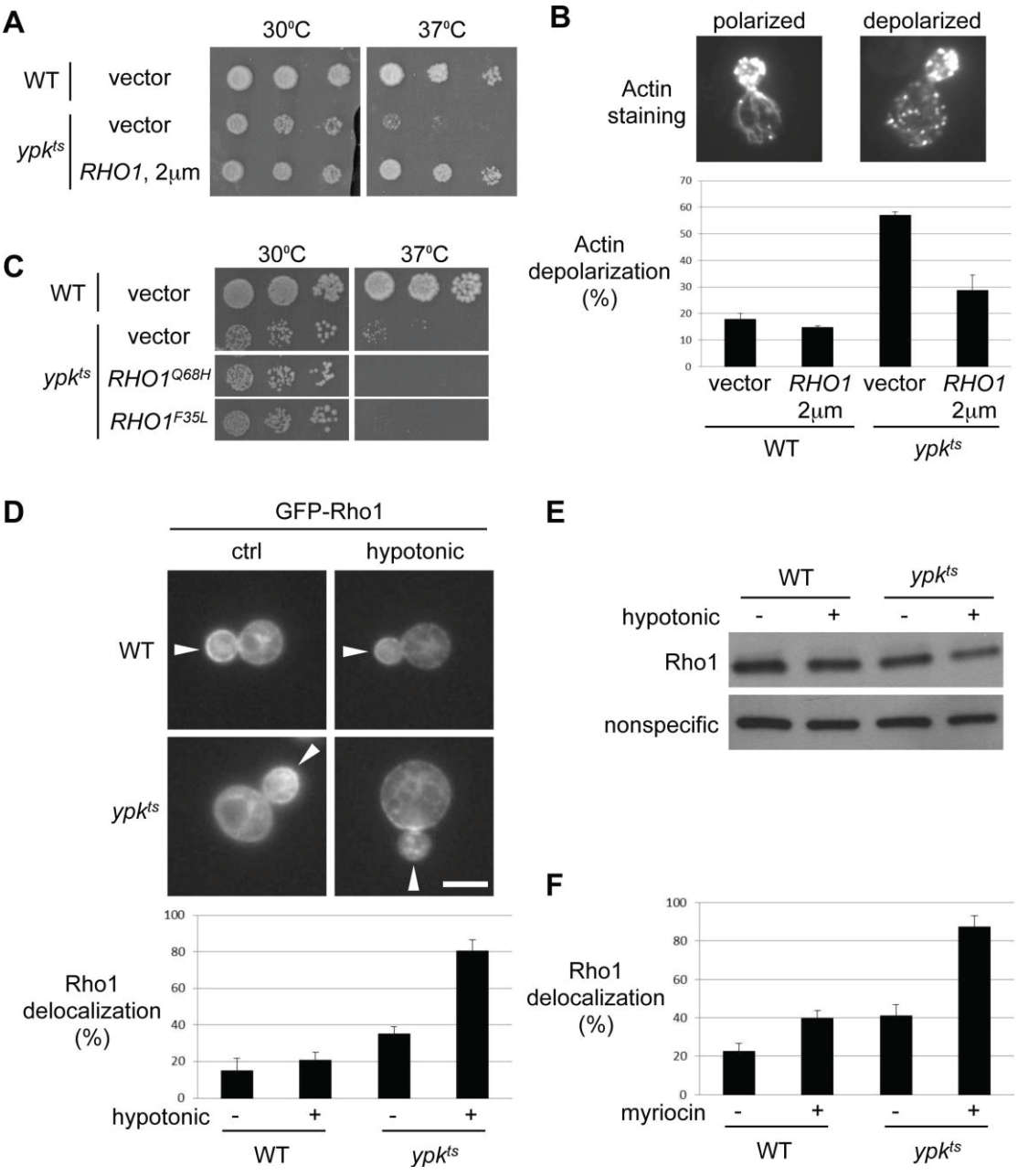

Fig. 1. Ypk1/Ypk2 regulate Rho1 localization.

(A) Growth rescue of the *ypk*^{ts} mutant by *RHO1* overexpression. Cells of the *ypk*^{ts} strain were grown at either permissive (30°C) or non-permissive (37°C) temperature for 3 days. (B)

Rescue of the actin polarization defect in the *ypk*^{ts} mutant by *RHO1* overexpression. Cells were grown at 30°C and then shifted to 37°C for 2 hours. The actin cytoskeleton was stained with Alexa Fluor 488-conjugated phalloidin. Representative images of polarized (WT) and depolarized (*ypk*^{ts}) actin are shown. In the chart, the percentage of small to medium-budded cells showing a depolarized actin cytoskeleton is shown. Data are presented as the mean ± SD of three independent experiments (n>50 cells were counted in each experiment). (C) Failure in growth rescue of *ypk*^{ts} mutant by *RHO1*^{Q68H} or *RHO1*^{F35L} expression. Cells were grown at either 30°C or 37°C for 4 days. (D) Effect of hypotonic shock on GFP-Rho1 localization. Cells were grown at 30°C and then shifted to 37°C for 2 hours. Images were taken 5 minutes after hypotonic shock. The percentage of small to medium-budded cells without Rho1 localization at the bud cortex is shown in the chart. Data are presented as the mean ± SD of three independent experiments (n>50 cells were counted in each experiment). Scale bar: 5 µm. (E) The protein expression level of Rho1. Cells were grown at 30°C and then shifted to 37°C for 2.5 hours. Cell lysates were prepared 10 minutes after hypotonic shock. Rho1 protein level was analysed using western blotting with anti-Rho1 antibody. Nonspecific signals are shown as a loading control. (F) Effect of myriocin on Rho1 localization. Cells were grown at 30°C and then treated with 0.5 µg/ml myriocin at 37°C for 2.5 hours. The percentage of small to medium-budded cells without Rho1 localization at the bud cortex is shown. Data are presented as the mean ± SD of three independent experiments (n>50 cells were counted in each experiment).

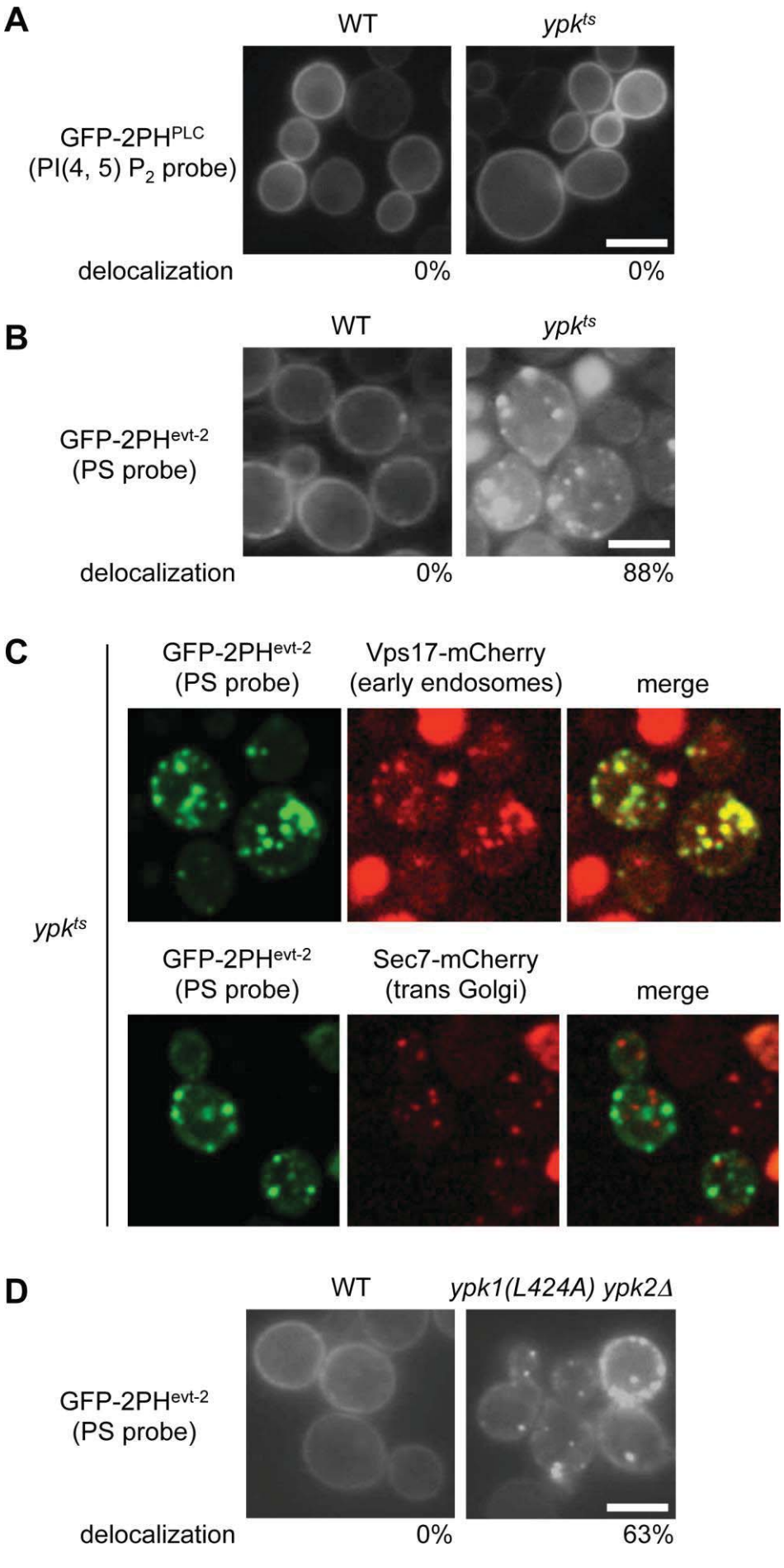

Fig. 2. Ypk1/Ypk2 regulate PS distribution.

(A) Localization of the GFP-2PH^{PLC} PI(4,5)P_2 probe after a 2 hour incubation at 37°C. The percentage of cells lacking a PM signal is shown (n>150 cells). Scale bar: 5 µm. (B) Localization of the PS probe GFP-2PH^{evt-2} after incubation for 2 hours at 37°C. The percentage of cells lacking a PM signal is shown (n>150 cells). Scale bar: 5 µm. (C) Co-localization analysis of the PS probe with the indicated organelle markers after 2 hours of incubation at 37°C. Adenine (0.07%) was added to the medium to prevent accumulation of the red pigment caused by *ade2* mutation. (D) Localization of the PS probe GFP-2PH^{evt-2} after 1NM-PP1 treatment for 5 minutes. The percentage of cells lacking PM signal is shown (n>50 cells). Scale bar: 5 µm.

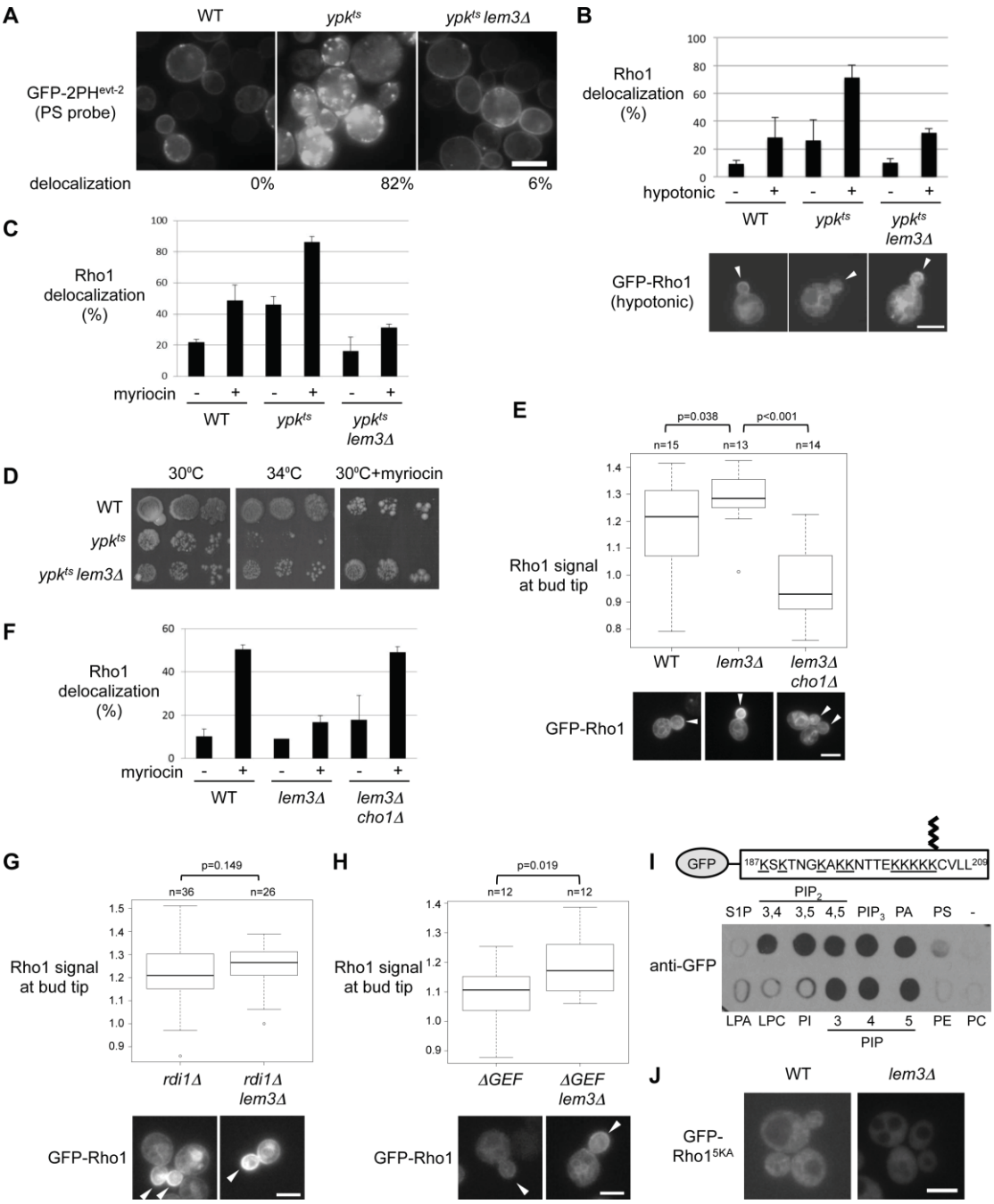

Fig. 3. PS contributes to Rho1 regulation through the Ypk1/Ypk2-flippase pathway.

(A) Rescue of PS distribution in the *ypk*^{ts} mutant by *LEM3* deletion. Cells were grown at 30°C and then shifted to 37°C for 2 hours. The percentage of cells lacking a PM signal is shown (n>150 cells). Scale bar: 5 µm. (B and C) Rescue of GFP-Rho1 localization in the *ypk*^{ts} mutant by *LEM3* deletion. In B, cells were grown at 30°C and then shifted to 37°C for 2 hours. Images were taken 5 minutes after hypotonic shock. Arrowheads indicate the cellular

growth site (bud tip). In C, cells were grown at 30°C and then treated with 0.5 µg/ml myriocin at 37°C for 2.5 hours. The percentage of small to medium-budded cells without Rho1 localization at the bud cortex is shown in the chart. Data are presented as the mean ± SD of three independent experiments (n>50 cells were counted in each experiment). Scale bar: 5 µm. (D) Growth rescue of the *ypk*^{ts} mutant by *LEM3* deletion. Cells of the *ypk*^{ts} strain were grown at either permissive (30°C) or non-permissive (34°C) temperature, or in the presence of 250 ng/ml myriocin for 5 days. (E) Enhanced cortical accumulation of GFP-Rho1 in the *lem3Δ* mutant and its suppression by *CHO1* deletion. The intensity of the GFP-Rho1 signal at the bud tip normalized by the mean intensity of the intracellular signal in buds is shown in the box plot. Representative cell images are shown. Arrowheads indicate the cellular growth site (bud tip). Scale bar: 5 µm. (F) Effect of myriocin on Rho1 localization. Cells were treated with 10 µg/ml myriocin for 2 hours. The percentage of small to medium-budded cells lacking Rho1 at the bud cortex is shown. Data are presented as the mean ± SD of three independent experiments (n>30 cells were counted in each experiment). Scale bars: 5 µm. (G and H) The effect of *LEM3* deletion on cortical localization of GFP-Rho1 in the absence of *RDI1* or three Rho1GEFs. The box plot shows the intensity of the GFP-Rho1 signal at the bud tip normalized by the mean intensity of the intracellular signal in buds. Representative cell images are shown. Because yeast cells lacking all three RhoGEFs (Rom1, Rom2, and Tus1) are lethal, Lrg1, a major Rho1 GAP, was also deleted in this experiment. Scale bar: 5 µm. (I) In vitro binding of the Rho1 PBS to membrane lipids. GFP-Rho1 PBS from yeast lysates was incubated with a PIP strips membrane (Echelon) and its affinity to specific lipids was analysed. (J) Diffused localization of GFP-Rho1-5KA. Scale bar: 5 µm.

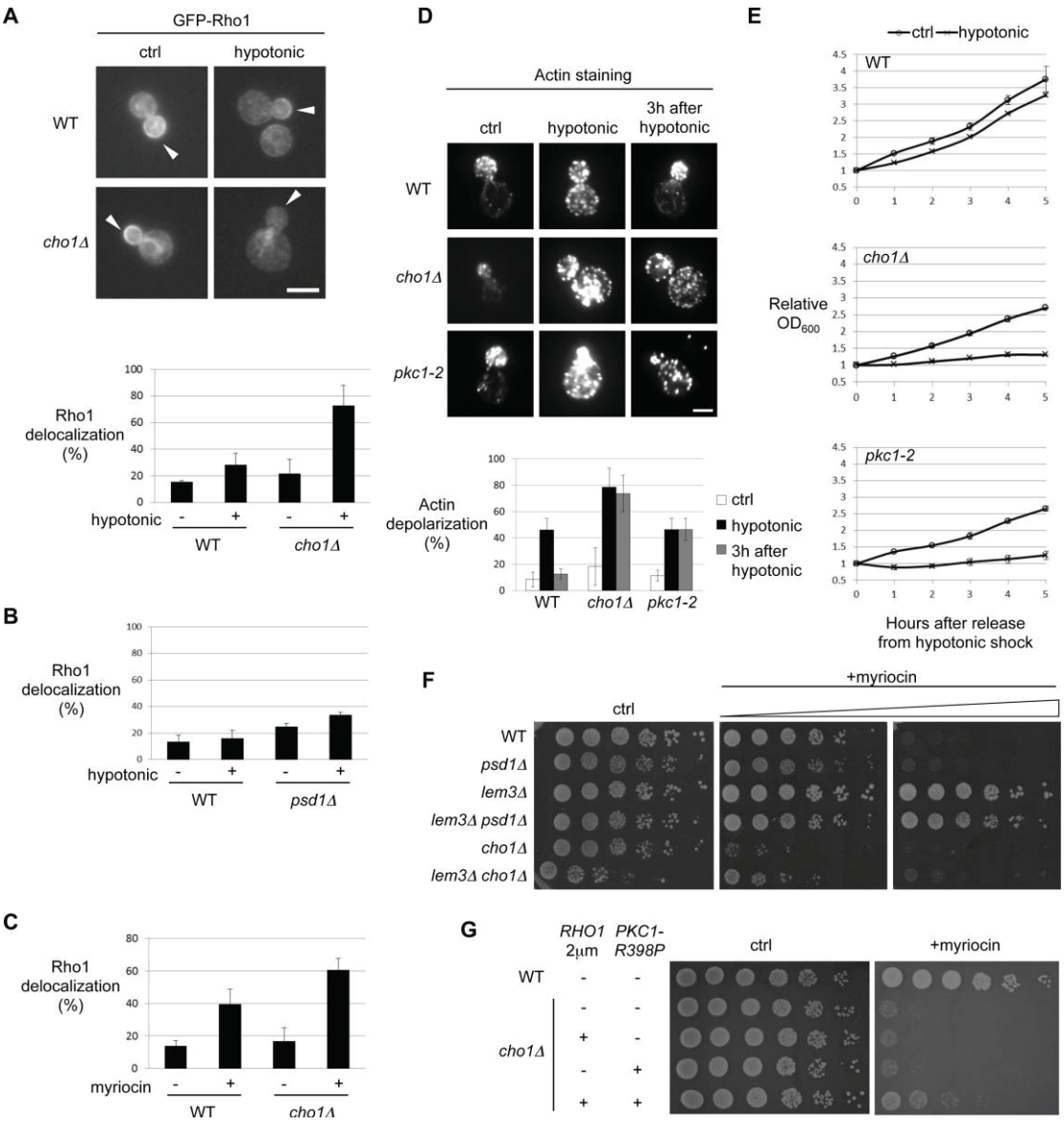

Fig. 4. PS is essential for recovery from PM stress.

(A and B) Effect of hypotonic shock on GFP-Rho1 localization. Images were taken 5 minutes after hypotonic shock. The percentage of small to medium-budded cells without Rho1 localization at the bud cortex is shown in the chart. Data are presented as the mean ± SD of three independent experiments (n>42 cells were counted in each experiment). Scale bar: 5 μm. (C) Effect of myriocin on Rho1 localization. Cells were treated with 1 μg/ml myriocin for 2.5 hours. The percentage of small to medium-budded cells without Rho1 localization at the bud cortex is shown. Data are presented as the mean ± SD of three independent experiments (n>41 cells were counted in each experiment). (D) Actin cytoskeleton after

hypotonic shock and its recovery after 3 hours. The indicated strains were grown at 40°C, exposed to transient (20 min) hypotonic shock and released to the medium containing 1 M sorbitol. Images were taken after staining actin with Alexa Fluor 488-conjugated phalloidin. Scale bar: 5 µm. The percentage of small to medium-budded cells showing a depolarized actin cytoskeleton is shown in the chart. Data are presented as the mean ± SD of three independent experiments (n>40 cells were counted in each experiment). (E) Cell proliferation with (cross) or without (circle) transient hypotonic shock performed as in (D). Data are presented as the mean ± SD of two independent experiments. (F) Growth of the indicated mutants in the presence of 500 or 1000 ng/ml myriocin. Cells were grown at 30°C for 2 days. (G) Growth of the indicated strains in the presence of 500 ng/ml myriocin. Cells were grown at 30°C for 3 days.

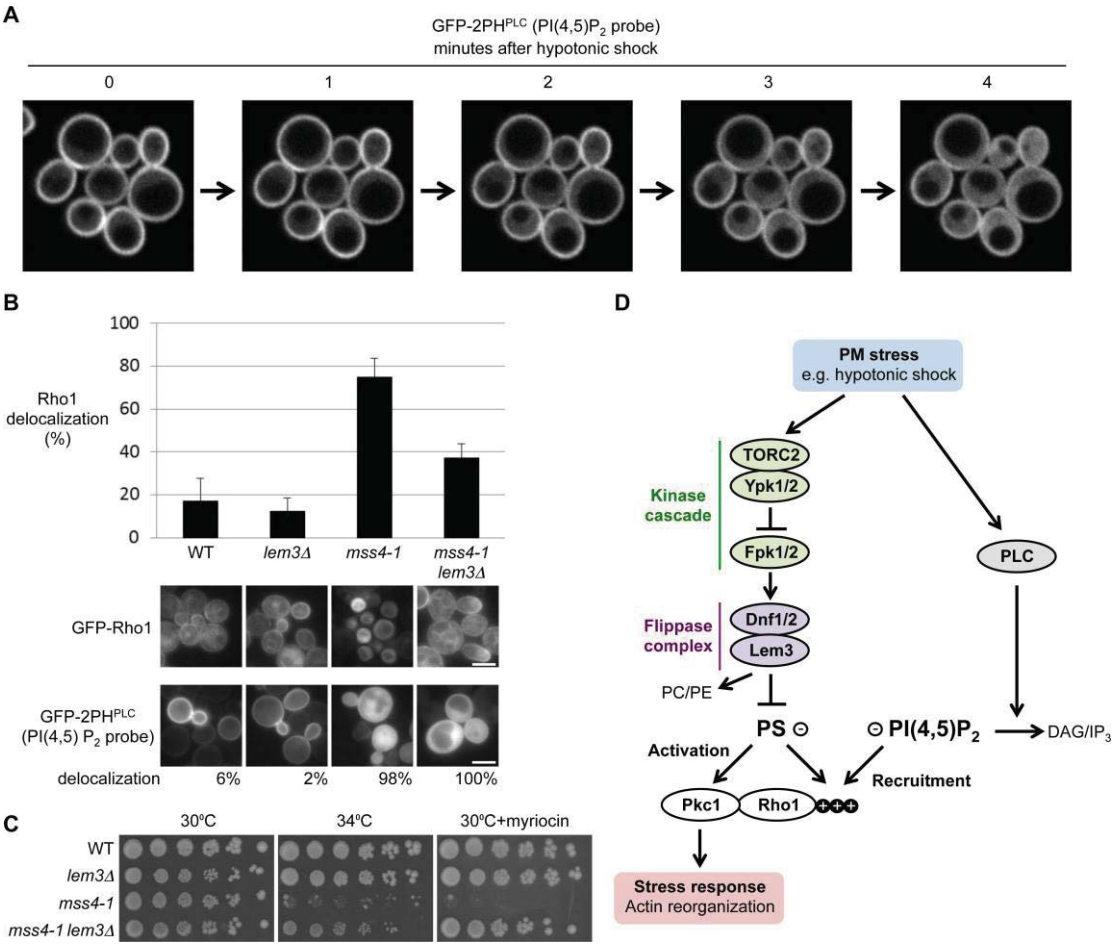

Fig. 5. Inhibition of the Lem3-containing flippase compensates for the loss of PI(4,5)P_2.

(A) Time-lapse imaging of PI(4,5)P_2 degradation upon hypotonic shock using the GFP-2PH^{PLC} P(4,5)IP_2 probe. (B) GFP-Rho1 localization after incubating for 3 hours at 37°C (top). The percentage of small to medium-budded cells lacking Rho1 at the bud cortex is shown. Data are presented as the mean ± SD of three independent experiments (n>26 cells were counted in each experiment). Representative cell images are shown. Localization of the GFP-2PH^{PLC} PI(4,5)P_2 probe after 2 hours of incubation at 37°C (bottom). The percentage of cells lacking PM localization is shown (n>46 cells). Scale bars: 5 µm. (C) Growth rescue of the *mss4-1* mutant by *LEM3* deletion. The *mss4-1* strain was grown at either a permissive (30°C) or non-permissive (34°C) temperature, or in the presence of 250 ng/ml myriocin for 5 days. (D) The schematic summary of Rho1 regulation in PM stress response.

Supplemental information

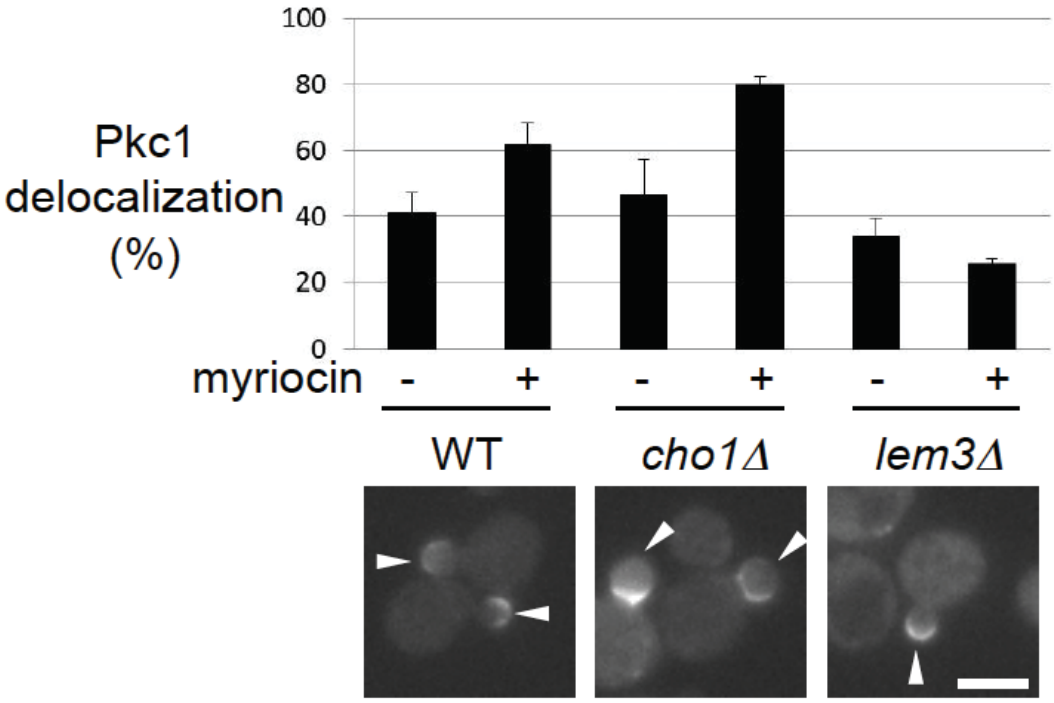

Figure S1, related to Figure 4 Effect of myriocin on Pkc1-GFP localization.

Cells were treated with 1 mg/ml myriocin for 2 hours. Percentage of small to medium-budded cells without Pkc1 localization at the bud cortex is shown. Data are presented as mean +/- SD from three independent experiments (n>58 cells were counted in each experiment). Representative cell images after myriocin treatment are shown. In all the images, arrowheads point to the cellular growth site (bud tip). Scale bars: 5 μm.

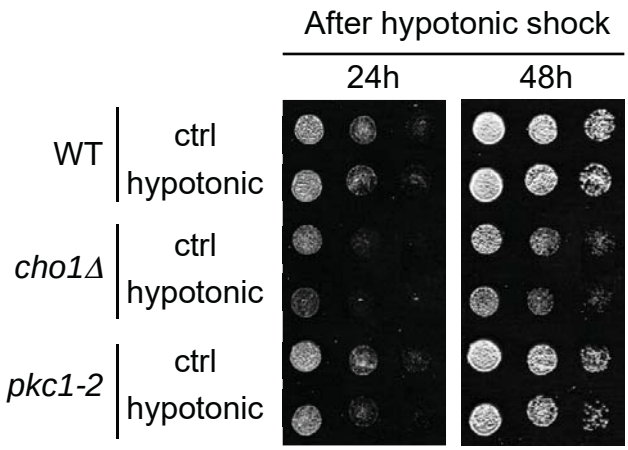

Figure S2, related to Figure 4 Long-term growth after hypotonic shock.

Recovery of cell growth after release from 20 minutes hypotonic shock as in the Fig. 3. Equal number of the cells were serially diluted and spotted on YPD containing 1M Sorbitol at 40°C. After 24 h, *cho1Δ* and *pkc1-2* strains exposed to hypotonic shock barely formed colonies, but they eventually formed equal number of the colonies after 48 h.

Table S1 Strains

Strain	Genotype	Source
BY4741	*MATa his3Δ1 leu2Δ0 met15Δ0 ura3Δ0*	Lab stock
RH310	BY4741 *cho1Δ::kanMX6*	This study
RH314	BY4741 *lem3Δ::kanMX6*	This study
RH376	BY4741 *lem3Δ::hphMX4 cho1Δ::kanMX6*	This study
RH701	BY4741 *psd1Δ::HIS3*	This study
RH702	BY4741 *lem3Δ::kanMX6 psd1Δ::HIS3*	This study
RH35	BY4741 *pkc1-2*	This study
SY1520	BY4741 *rdi1Δ::HIS3MX6*	This study
RH549	BY4741 *rdi1Δ::HIS3MX6 lem3Δ::kanMX6*	This study
SY1416	BY4741 *rom1Δ::kanMX6 rom2Δ::kanMX6 tus1Δ::kanMX6 lrg1Δ::HIS3MX6*	Yoshida et al., 2009
RH384	BY4741 *rom1Δ::kanMX6 rom2Δ::kanMX6 tus1Δ::kanMX6 lrg1Δ::HIS3MX6 lem3Δ::hphMX4*	This study
YOC807	*MATa ade2 leu2 lys2 trp1 ura3 mss4::HIS3 ade3::MSS4::LEU2*	Homma et al., 1998
YOC808	*MATa ade2 leu2 lys2 trp1 ura3 mss4::HIS3 ade3::mss4-1::LEU2*	Homma et al., 1998
RH354	YOC807 *lem3Δ::kanMX6*	This study
RH357	YOC808 *lem3Δ::kanMX6*	This study
YPH499	*MATa ade2-101^{Ochre} his3Δ200 leu2Δ1 lys2-801^{amber} trp1Δ63 ura3-52*	Roelants et al., 2010
YPT40	YPH499 *ypk1-1^{ts}::HIS3 ypk2Δ1::TRP1*	Roelants et al., 2010
RH483	YPT40 *lem3Δ::kanMX6*	This study
yAM123A	BY4741 *ypk1(L424A)::URA3 ypk2Δ::kanMX4*	Gifted from Jeremy Thorner
RKH1	YPT40 *SEC7-mCherry::natMX4*	This study
RKH2	YPT40 *VPS17-mCherry::natMX4*	This study

Table S2 Plasmids

Plasmid	Gene	Source
SP301	*CEN URA3 GFP-RHO1*	Yoshida et al., 2009
pRH210	*CEN URA3 PKC1-GFP*	This study
pRH176	*2um URA3* P_{PRC1}*-GFP-2PH*^{PLC}	Stefan et al., 2002
SP353	*2um LEU2* P_{GAL1}*-GFP-RHO1*$^{187-209}$	This study
pRH241	*CEN URA3 GFP-RHO1*^{5KA}	This study
pRS316	*CEN URA3* empty vector	Sikorski et al., 1989
YEP352-RHO1	*2um URA3 RHO1*	Gifted from Daniel Lew
pRS315	*CEN LEU2* empty vector	Sikorski et al., 1989
SP336	*CEN LEU2 HA-RHO1*^{Q68H}	Yoshida et al., 2009
SP335	*CEN LEU2 HA-RHO1*^{F35L}	Yoshida et al., 2009
pYO1775	*CEN LEU2 PKC1-R398P*	Nonaka et al., 1995
pAGX-h-evt2-2*PH	*CEN URA3 GFP-2PH*$^{evt-2}$	Uchida et al., 2011
p415-GFP-h-evt2-2*PH	*CEN LEU2 GFP-2PH*$^{evt-2}$	This study

Supplemental Reference

Sikorski, RS. et al., (1989) A system of shuttle vectors and yeast host strains designed for efficient manipulation of DNA in Saccharomyces cerevisiae. Genetics 122:19-27